Mechanism analysis of tartrazine biosorption onto masau stones; a low cost by-product from semi-arid regions

Albadarin, A., Charara, M., Tarboush, B. J. A., Walker, G., Kurniawan, T. A., Ahmad, M., Naushad, M., & Mangwandi, C. (2017). Mechanism analysis of tartrazine biosorption onto masau stones; a low cost by-product from semi-arid regions. *Journal of Molecular Liquids*, *242*, 478-483. https://doi.org/10.1016/j.molliq.2017.07.045

Published in:
Journal of Molecular Liquids

Document Version:
Peer reviewed version

Mechanism analysis of tartrazine biosorption onto masau stones; a low cost by-product from semi-arid regions

Ahmad B. Albadarin[1,2*], M. Charara[3], B.M. Abu Tarboush[3], M.N.M Ahmad[3], Tonni Agustiono Kurniawan[4], Mu Naushad[5], G.M. Walker[1] and C. Mangwandi[2]

[1]*Department of Chemical and Environmental Science, Bernal Institute, University of Limerick, Limerick, Ireland.*
[2]*School of Chemistry and Chemical Engineering, Queen's University Belfast, Belfast BT9 5AG, Northern Ireland UK.*
[3]*Faculty of Engineering and Architecture American University of Beirut, Beirut, Lebanon.*
[4]*College of Ecology and Environment, Xiamen University, Xiamen 361102 Fujian Province, PR China.*
[5]*Department of Chemistry, College of Science, King Saud University, Riyadh-11451, Saudi Arabia.*

Abstract

The removal of tartrazine from aqueous solutions using masau stone (MS) as a novel low-cost biosorbent was investigated. The impact of several influential parameters such as; initial pH, contact time, initial concentration and temperature on the biosorption process of tartrazine was studied and optimized. The mechanisms of tartrazine removal by the MS biosorbent and their kinetics and isotherm studies are also presented. It was observed that the efficiency of the removal of tartrazine depends on the pH of the solution and the maximum efficiency (approx. 87% at C_o = 100) was found at pH 2. Kinetic studies were well suited and found to be in good agreement with the pseudo-second order model. The biosorption equilibrium data was adequately described by the Langmuir isotherm model at 20 °C and 30 °C. High temperatures seem to promote multilayer biosorption as the tartrazine experimental data best fits both Freundlich and Redlich-Peterson isotherms (R^2 = 0.996 for both). The maximum biosorption capacities of tartrazine were between; 0.096 mmol/g (51.3 mg/g) at 20 °C and 0.126 mmol/g (65.1 mg/g) at 60 °C. The thermodynamic parameters obtained indicated a positive and low value of ΔH°, suggesting an endothermic and physical nature process with biosorption mechanisms related to H-bonds, van der Waals and electrostatic interactions. The results clearly indicated that masau stone would be a suitable biosorbent for the anionic dye, tartrazine, from contaminated wastewater under specific conditions.

Keywords: *Azo Dye; Tartrazine; Masau Biomass; By-Products; Biosorption; Wastewater treatment.*

*Correspondence author: Email: Ahmad.B.Albadarin@ul.ie

1. Introduction

The discharge of effluents that contain synthetic dyes is a major concern to the environment and aquatic life due to the hazards associated with toxicity and the large quantity of dye-loaded wastewater released [1-3]. For instance, the textile industry alone manufactures an extraordinary 60 billion kgs of fabric per annum, using up to 9×10^{12} gallons of water. About 10–25% of textile dyes could not be recovered during the dyeing process, and 2–20% is discharged as aqueous effluents into different environmental components with an estimated 800,000 tons of synthetic dyes produced each year and ~50% of these classified as azo dyes [4-6]. Many of these synthetic dyes and their breakdown products released are carcinogenic or mutagenic to life forms, primarily due to carcinogens such as naphthalene, benzidine, and other aromatic compounds [4]. Also, most of these dyes have a recalcitrant and inhibitory nature because of their large size and complex molecular structures and are thus considered non-oxidizable by conventional physical and biological treatments. For these reasons, a large number of recent studies have been focused on the elimination and treatment of dye-bearing effluents. Various methods such as coagulation/flocculation, adsorption/biosorption, ion-exchange and chemical precipitation have been employed for the treatment of dye-polluted water [7-11]. A biosorption-based treatment process provides a number of advantages when compared to the conventional technologies utilized, especially when using cheap and readily available biosorbents. These biosorbents can be produced using inexpensive growth media or obtained as a by-product from industry. Biosorption has many beneficial features including; the selective removal of ions/molecules over a broad range of temperatures and pH values, a negligible amount of chemical/biological sludge, its fast kinetics of adsorption and desorption (possibility of biosorbent regeneration) and low capital and operation cost [1, 8, 12-15]. Recently, the search for low-cost materials which are able to remove unwanted pollutants from contaminated water has intensified [16]. Materials locally available in large quantities such as

agricultural wastes or industrial by-products may be used as low-cost adsorbents with little or no processing. Their use as an adsorbent for water purification would not only add to their economic value, but also help industries reduce the cost of waste disposal and provide a potential alternative to activated carbon [17]. Thus, in this study, masau stone by-products have been used for the biosorption of an ionic dye from aqueous solutions. The masau (Ziziphus mauritiana) tree typically grows in arid and semi-arid regions around the world. Its fruit is one of the most commonly utilized wild fruits in Zimbabwe. Extracts from the fruits, roots, leaves, seeds, and bark of the masau tree are utilized as traditional medicines to treat the effects of skin diseases, inflammatory conditions, insomnia and fever. For these reasons, the masau tree plays an important role in the integrated economy of arid regions [18]. To date, there are no systematic studies of the use of masau fruits and shells in the removal of pollutants, despite the large quantities of waste product generated as a result of processing the fruit. Tartrazine (TZ) is a major contaminant in the environment. Tartrazine, a coal tar derivative, is a very popular azo dye extensively used in food-stuffs, medicines, cosmetics and textile manufacturing [19]. Due to the hydrophilic nature of tartrazine, its presence can be noticed as a yellow menace in effluents. Contact with the dye results in many kinds of health issues including: skin eczema, hypersensitivity, allergies, asthma, mutagenic and carcinogenic effects and immunosuppressive effects [5]. The studies dealing with the removal of tartrazine (TZ) using raw biosorbents such as masau stone (MS) are rare and therefore, tartrazine was selected as a model dye. The key aims of the current investigation are to (i) examine the effect of influential factors including solution pH, initial dye concentration and contact time on the biosorption process, and (ii) determine the mechanism of TZ biosorption onto MS and the type of TZ–MS interactions occurring by applying a range of equilibrium and kinetic models and analytical techniques to the biosorption experimental data.

2. Materials and methods

2.1. Masau stone biosorbent

Masau stone (MS) biomass, was collected and mechanically crushed. After which, the biosorbent was repeatedly washed with boiled water and finally with distilled water, and dried at 110 ºC for 24 hrs. After sieving, approx. 70% of MS particles had a mean diameter in the range of 350 – 500µm. This particle size was therefore used for the biosorption experiments. The specific surface area of masau stone was measured by the N_2-BET method as 27.66 m^2/g.

2.2. Methods

Tartrazine (534.3 g/mol) was purchased from Sigma Aldrich, UK. All chemicals were of analytical grade and used without further purification. Hydrochloric acid (HCl) and sodium hydroxide (NaOH) were used for the pH adjustment. Synthetic tartrazine stock solution was prepared with distilled water (resistivity 18.24 Ωcm). Batch biosorption studies were performed in a series of 50 cm^3 glass jars on a mechanical shaker. For each experimental point, 25 cm^3 of a stock solution was first added into the glass jar and then the masau stone biosorbent was added and maintained under shaking in a regulated speed shaker (100 rpm, biomass dosage 4.0 g/dm^3 and 20°C for 96 hrs). After the biosorption, the samples were filtered and analysed for tartrazine concentration. The biosorption process was studied as a function of pH (2–11) with C_o of 0.187 mM and biomass dosage 4.0 g/dm^3, initial tartrazine concentration (0.057-0.861 mM) and contact time. After reaching equilibrium, the concentration of tartrazine in the aqueous solution was analysed by UV analysis, performed on a UV-Visible spectrophotometer (Perkin Elmer LAMBDA 25, UK) at a maximum wavelength λ_{max} = 426 nm.

Tartrazine (TZ) uptake, q (mmol/g), and percentage of removal (%) were calculated according to Eq. (1) and (2), respectively:

$$q = \left[\frac{C_o - C_e}{M}\right] \times V \qquad (1)$$

$$\text{The removal efficiency (\%)} = \left[1 - \frac{C_e}{C_o}\right] \times 100\% \qquad (2)$$

where C_o and C_e are the initial and equilibrium concentrations of tartrazine (TZ) in mM, M is the amount of dry biomass in grams and V is the volume of the tartrazine (TZ) solution in dm^3.

3. Results and discussion

3.1. pH experiment

The pH of the solution has a critical role when it comes to controlling the dissociation of different functional groups on the biosorbent active sites, as well as its surface charge, and the extent of ionization of the adsorbate in the solution [20]. The effect of initial solution pH on the removal of tartrazine was carried out in the range of 2–11 as illustrated in Figure 1. Biosorption of TZ by masau stone biomass was particularly dependent on the pH of the dye solution. At a pH value of around 2, the masau stone (MS) surface is more positively charged through increased functional groups protonation, than at higher pH values. The removal efficiency decreased from 87% to 15% when the solution pH was increased from 2.18 to 11.0, following typical anionic adsorption/biosorption behaviour. The mechanisms of the biosorption process of TZ onto MS were mainly due to the electrostatic attractions of the tartrazine molecules with protonated functional groups such as hydroxyl, carbonyl and amine groups of the masau stone at $pH < pH_{PZC}$. Conversely, at higher pH, the number of protonated functional groups decreases and more OH^- ions compete with anionic dye ions for the biosorption sites. At alkaline pH, the covalent coordination bonds between sodium ions and the surface functional group of masau stone, such as carboxylic and sulfonic acid are very weak in basic condition. As a result, the number of protonated functional groups decreases and more OH^- ions compete with the anionic ions of the adsorbate for the sorption sites, leading to a lower removal of tartrazine by the adsorbent. Similar trends were reported for the removal of tartrazine using hen feathers [19], activated carbon biosorbents of Lantana camara [21] and

Spirulina platensis [22]. Therefore, pH 2 was used for subsequent runs of the biosorption experiments.

3.2. Biosorption kinetics

The biosorption kinetics are used for the determination of the rate controlling mechanism of biosorption processes such as; biosorption on surface and chemical reaction or diffusion mechanisms. The pseudo-first order kinetic model assumes that the rate of change in the solute concentration over time is logarithmic proportional to changes in the saturation concentration and the amount of absorbent over time [23, 24]. The pseudo-first order model equation is given as follows [25]:

$$q_t = q_e\left(1 - e^{-k_1 t}\right) \tag{3}$$

The pseudo-second order equation is given as [26]:

$$q_t = \frac{k_2 q_e^2}{\left(1 + k_2 q_e t\right)} t \tag{4}$$

where k_1 is the pseudo-first order kinetic constant (1/min) and k_2 is the constant of the pseudo-second order kinetics (g (mmol/min)).

The results of the kinetic biosorption studies are shown in Figure 2. The parameters of the kinetics equations are given in Table 1. The most accurate model was considered based on the determination coefficient (R^2). It can be observed that the kinetics of TZ removal by masau stone followed the pseudo-second order model for the seven TZ initial concentrations employed in the present study. These results suggested that the pseudo-second order biosorption mechanisms are predominant. Furthermore, the nonlinear relationship between the initial dye concentration and the rate constant indicates that mechanisms such as; ion exchange, chelation and physical adsorption may be involved in the biosorption process.

It is very important to realise that adsorption/biosorption mechanisms (chemical bonding or chemisorptions) cannot simply be determined based on carrying out kinetic experiments or by fitting kinetic models. In this case, analytical methods and/or adsorptive thermodynamic data (i.e., changes in enthalpy and entropy) and activation energies, are essential to confirm that the removal process is either physical or chemical.

The intra-particle diffusion model was used to investigate the mechanism involved in the biosorption process. Assuming that the rate is controlled by pore and intra-particle diffusion, the amount biosorbed (q_t) is proportional to the square root of time ($t^{0.5}$) in a non-flow-agitated system, according to the relationship given by Weber and Morris [27]:

$$q_t = k_{id} \times t^{0.5} + C_{id} \quad (5)$$

k_{id} (mg/g.min$^{0.5}$) is the intra-particle diffusion rate constant and C_{id} is proportional to the boundary layer thickness.

The intra-particle diffusion model [28] was plotted in order to verify the influence of mass transfer resistance on the binding of TZ to the masau stone (Table 2 and Figure 3). Thus, the intra-particle diffusion constant, k_{id} (mg/g.min$^{0.5}$), can be obtained from the slope of the plot of q_t (uptake at any time, mg/g) versus the square root of time. If this plot passes through the origin, then intra-particle diffusion is the rate controlling step. Figure 3 shows the plots of q_t *versus* $t^{0.5}$, with multi-linearity though, none of the plots passed through the origin ($C_{id} \neq 0$), which implies that the process involves more than one kinetic stage (or sorption rate); external surface biosorption or the instantaneous biosorption stage is not the main rate controlling step [28, 29]. It can be seen from Table 2 that the values of k_{id} increase with the increase of initial dye concentration. This is due to the effect of potential force as a result of the gradual change in concentration.

3.3. Biosorption isotherm at various temperatures

Since the equilibrium isotherm is of vital importance to the adsorption system for the removal of dye from an aqueous solution, it is essential to establish the most suitable correlation for the equilibrium curves [20, 30]. In this study, three of the most commonly used models: Langmuir [31], Freundlich [32] and Redlich-Peterson [33], were employed to describe the equilibrium isotherm of the dye removal experiment. Linear forms of isotherm models are unable to provide a fundamental understanding of the ion adsorption systems, resulting in improper conclusions. Therefore, non-linear regression in SigmaPlot11 was used to fit the isotherm models to the experimental data at different solution temperatures and the summary of the fits is presented in Table 3 and Figure 4. There was an initial increase in the amount of biosorbed dye per unit mass of MS, but that amount later started following a plateau evolution at higher solution concentrations. At 20 ºC, the q_{max} value was measured as 0.096 mmol/g; this is equivalent to approx. 51.3 mg/g. Also, it is found that the tartrazine experimental data best fits both Langmuir and Redlich-Peterson isotherms (R^2 = 0.986 and 0.985, respectively) with the Redlich-Peterson constant value, β, close to unity (0.835). This specifies a homogeneous surface binding and that the Redlich–Peterson isotherm is approaching the Langmuir form and not the Freundlich isotherm [34]. It is also shown in Table 3 that, at 20 ºC, the magnitude of the Langmuir constant b was 6.460 dm^3/mmol. The maximum biosorption capacity 20 ºC was found to be 0.096 mmol/g. The $1/n$ value shown in Table 3 for the Freundlich model indicates that the strength of the biosorption process is related to the distribution of energy sites. In real life, wastewater from different industries is discharged at a wide range of temperatures based on the process that generates the effluents. Accordingly, studying the effect of temperature on dye adsorption is very crucial. The effect of temperature increase on the biosorption isotherm equilibrium is presented in Table 3. Increasing the temperature from 20 to 60 ºC increased the values of the Langmuir constants, b and q_{max}, and K_F with a more pronounced increase in the

value of *b*. This reflects the endothermic nature of the biosorption of TZ molecules on the surface of the MS. This increase in biosorption capacity at high temperature might be due to more available sites for biosorption and strong interaction forces between the TZ dyes molecules and the MS surface. On the other hand, a slight decrease in the values of *1/n* and the Redlich-Peterson constant value, *β,* are found as a result of increasing the temperature. High temperatures seem to promote multilayer biosorption as the tartrazine experimental data best fits both Freundlich and Redlich-Peterson isotherms (R^2 = 0.996 for both). A brief comparison of the q_{max} values obtained in this study to other materials is presented in Table 4 [19, 22, 35-37]. The biosorption capacity of TZ onto masau stone is average among the materials listed. However, the use of the masau biosorbent for anionic dye removal is very promising since it is cheap and readily available in many countries.

3.4. Thermodynamic parameters

In order to better understand the nature and mechanism of the TZ dyes biosorption onto the MS surface, biosorption data at different temperatures, were used to calculate thermodynamic parameters such as change in enthalpy (ΔH°), change in free Gibbs energy (ΔG°) and change in entropy (ΔS°) Eqs. (6) to (8):

$$\Delta G^o = -RT \ln 55.5 \times b \times 1000 \quad (6)$$

$$\Delta G^o = \Delta H^o - T\Delta S^o \quad (7)$$

$$\ln 55.5 \times b \times 1000 = \frac{\Delta S^o}{R} - \frac{\Delta H^o}{R}\frac{1}{T} \quad (8)$$

where *R* is the universal gas constant (8.314 J/mol K). The term 55.55 (mol/dm^3) × *b* (dm^3/mmol) × 1000 is dimensionless.

The above equation was used to find the slope and intercept which represent the values of (ΔH°) and (ΔS°) respectively. Estimated thermodynamic parameters, change in enthalpy (ΔH°), change in free Gibbs energy (ΔG°) and change in entropy (ΔS°) are presented in Table 5. The endothermic nature of this system is confirmed by the positive value of ΔH°. Negative

values of ΔG° and positive values of ΔS° and ΔH° indicate that the biosorption process is spontaneous. Moreover, the increase in temperature reduced the values of ΔG° which emphasize the spontaneity of the biosorption process at a high temperature. Upon increasing the temperature, the absolute values of ΔG° increased, indicating that the biosorption also increased. This finding agrees with the reported values of biosorption capacity at different temperatures in Table 3. Additionally, it can be observed that the energies involved in the process (≈13 kJ/mol) are within the range of the intermolecular interactions characteristic binding energy of physical bonding: hydrogen bonds (4–13 kJ/mol) and electrostatic attractions (6–80 kJ/mol).

3.5. FTIR and SEM analysis

The occurrence of moderately negatively charged groups in the tartrazine structure, such as COOH, SO_3, and OH allows the formation of columbic forces, hydrogen bonds, covalent bonds or weak van der Waals forces [38]. The FTIR, Figure 5, shows a number of absorption peaks suggesting complex properties of biosorption capabilities of masau. The dominant peak at 3500 1/cm is attributed to both surface hydroxyl (OH) stretching of carboxylic groups and also stretching of amide groups (–NH) [39]. These groups are significantly involved in the hydrogen bonds. The peak at 2950 1/cm is attributed to the alkyl group (C–H) while the peak at 1750 1/cm is attributed to the carbonyl group (C=O). A slight shift in the peaks within the alkyl group from 1743 to ~1741 1/cm is attributed to biosorption of dye molecules. On the fresh masau stone, the N–C=O stretch peak occurs at 1650 1/cm, and is absent after biosorption, suggesting that the amide group might have been involved in the biosorption. The absorption at 870 1/cm may be related to the C–H rocking vibrations of cellulose. A new peak appears at 1635 1/cm after biosorption. The peaks in the range of 950–1200 1/cm may represent the C–O stretching group. The spectra also show that some peaks in the range 455 to 555 1/cm that were present in the masau prior to biosorption were not present after biosorption. Consequently,

the FTIR shows the availability of these different function groups that will contribute to the biosorption of TZ. The FTIR also suggests that all the intensities of the peaks are reduced due to the biosorption of TZ on the surface and inside the pores of the biosorbent. The mechanisms of TZ biosorption may be due to the positive charge of the dye and the hydrophobic character of the TZ molecules. Thus, the mechanisms of TZ biosorption are due to the electrostatic attraction between the functional groups and TZ. The SEM of both fresh and TZ loaded masau are shown in Figure 6. There is evidence to suggest that the surface has been changed due to the biosorption of TZ. It is also shown that the biosorbed TZ tends to make the MS morphology structures less defined.

4. Conclusion

In this investigation, detailed results were presented for biosorption of tartrazine (TZ) from aqueous solutions using masau stone (MS). The results showed that the removal of TZ onto MS fluctuates very little in the pH range of 4–12 but decreases with pH value as pH exceeds 2. The Langmuir isotherm model was found to fit well to the experimental data as compared to other applied isotherm models. The maximum biosorption capacity of TZ biosorbed was 0.126 mmol/g at 60 °C. The kinetic study showed that the pseudo-second order model is suitable for describing the experimental data and that the external surface biosorption stage is not the main rate controlling step and film diffusion might be implicated in the sorption process.

5. References

[1] A.B. Albadarin, J. Mo, Y. Glocheux, S. Allen, G. Walker, C. Mangwandi, Preliminary investigation of mixed adsorbents for the removal of copper and methylene blue from aqueous solutions, Chemical Engineering Journal, 255 (2014) 525-534.

[2] B. Heibati, S. Rodriguez-Couto, N.G. Turan, O. Ozgonenel, A.B. Albadarin, M. Asif, I. Tyagi, S. Agarwal, V.K. Gupta, Removal of noxious dye—Acid Orange 7 from aqueous solution using natural pumice and Fe-coated pumice stone, Journal of Industrial and Engineering Chemistry, 31 (2015) 124-131.

[3] A.A. Alqadami, M. Naushad, M.A. Abdalla, M.R. Khan, Z.A. Alothman, Adsorptive Removal of Toxic Dye Using Fe3O4–TSC Nanocomposite: Equilibrium, Kinetic, and Thermodynamic Studies, Journal of Chemical & Engineering Data, 61 (2016) 3806-3813.

[4] Zaharia Carmen, S. Daniela, Textile organic dyes – characteristics, polluting effects and separation/elimination procedures from industrial effluents – a critical overview, www.intechopen.com, 3 (2012) 55-86.

[5] S. Banerjee, M.C. Chattopadhyaya, Adsorption characteristics for the removal of a toxic dye, tartrazine from aqueous solutions by a low cost agricultural by-product, Arabian Journal of Chemistry, 10 (2017) 1629-1638.

[6] P. Geetha, M.S. Latha, M. Koshy, Biosorption of malachite green dye from aqueous solution by calcium alginate nanoparticles: Equilibrium study, Journal of Molecular Liquids, 212 (2015) 723-730.

[7] E. Fosso-Kankeu, H. Mittal, S.B. Mishra, A.K. Mishra, Gum ghatti and acrylic acid based biodegradable hydrogels for the effective adsorption of cationic dyes, Journal of Industrial and Engineering Chemistry, 22 (2015) 171-178.
[8] A.B. Albadarin, C. Mangwandi, Mechanisms of Alizarin Red S and Methylene blue biosorption onto olive stone by-product: Isotherm study in single and binary systems, Journal of Environmental Management, 164 (2015) 86-93.
[9] K.L. Yeap, T.T. Teng, B.T. Poh, N. Morad, K.E. Lee, Preparation and characterization of coagulation/flocculation behavior of a novel inorganic–organic hybrid polymer for reactive and disperse dyes removal, Chemical Engineering Journal, 243 (2014) 305-314.
[10] B. Makhoukhi, M.A. Didi, H. Moulessehoul, A. Azzouz, D. Villemin, Diphosphonium ion-exchanged montmorillonite for Telon dye removal from aqueous media, Applied Clay Science, 50 (2010) 354-361.
[11] I. Anastopoulos, G.Z. Kyzas, Progress in batch biosorption of heavy metals onto algae, Journal of Molecular Liquids, 209 (2015) 77-86.
[12] A.B. Albadarin, A.a.H. Al-Muhtaseb, N.A. Al-laqtah, G.M. Walker, S.J. Allen, M.N.M. Ahmad, Biosorption of toxic chromium from aqueous phase by lignin: mechanism, effect of other metal ions and salts, Chemical Engineering Journal, 169 (2011) 20-30.
[13] A.B. Albadarin, Y. Glocheux, M.N.M. Ahmad, G.M. Walker, C. Mangwandi, Novel comparison of kinetic models for the adsorption-coupled reduction of Cr(VI) using untreated date pit biomaterial, Ecological Engineering, 70 (2014) 200-205.
[14] A.B. Albadarin, C. Mangwandi, G.M. Walker, S.J. Allen, M.N.M. Ahmad, M. Khraisheh, Influence of solution chemistry on Cr(VI) reduction and complexation onto date-pits/tea-waste biomaterials, Journal of Environmental Management, 114 (2013) 190-201.
[15] A.B. Albadarin, C. Mangwandi, G.M. Walker, S.J. Allen, M.N. Ahmad, Biosorption characteristics of sawdust for the removal of Cd(II) Ions: Mechanism and thermodynamic studies, Chemical Engineering Transactions, 24 (2011) 1297-1302.
[16] T.A. Kurniawan, G.Y.S. Chan, W.-h. Lo, S. Babel, Comparisons of low-cost adsorbents for treating wastewaters laden with heavy metals, Science of The Total Environment, 366 (2006) 409-426.
[17] S. Babel, T.A. Kurniawan, Cr(VI) removal from synthetic wastewater using coconut shell charcoal and commercial activated carbon modified with oxidizing agents and/or chitosan, Chemosphere, 54 (2004) 951-967.
[18] J.F. Morton, Fruits of warm climates, Indian jujube. in J. F. Morton, (ed.), Florida: Miami (1987) 272–275.
[19] A. Mittal, L. Kurup, J. Mittal, Freundlich and Langmuir adsorption isotherms and kinetics for the removal of Tartrazine from aqueous solutions using hen feathers, Journal of hazardous materials, 146 (2007) 243-248.
[20] B. Heibati, M. Ghoochani, A.B. Albadarin, A. Mesdaghinia, A.S.H. Makhlouf, M. Asif, A. Maity, I. Tyagi, S. Agarwal, V.K. Gupta, Removal of linear alkyl benzene sulfonate from aqueous solutions by functionalized multi-walled carbon nanotubes, Journal of Molecular Liquids, 213 (2016) 339-344.
[21] R.K. Gautam, P.K. Gautam, S. Banerjee, V. Rawat, S. Soni, S.K. Sharma, M.C. Chattopadhyaya, Removal of tartrazine by activated carbon biosorbents of Lantana camara: Kinetics, equilibrium modeling and spectroscopic analysis, Journal of Environmental Chemical Engineering, 3 (2015) 79-88.
[22] G.L. Dotto, M.L.G. Vieira, V.M. Esquerdo, L.A.A. Pinto, Equilibrium and thermodynamics of azo dyes biosorption onto Spirulina platensis, Brazilian Journal of Chemical Engineering, 30 (2013) 13-21.
[23] M. Kitis, E. Karakaya, N.O. Yigit, G. Civelekoglu, A. Akcil, Heterogeneous catalytic degradation of cyanide using copper-impregnated pumice and hydrogen peroxide, Water Research, 39 (2005) 1652-1662.
[24] A.B. Albadarin, M.N. Collins, M. Naushad, S. Shirazian, G. Walker, C. Mangwandi, Activated lignin-chitosan extruded blends for efficient adsorption of methylene blue, Chemical Engineering Journal, 307 (2017) 264-272.
[25] S. Lagergren, About the theory of so-called adsorption of soluble substances, Kungliga Svenska Vetenskapsakademiens Handlingar 24 (1898) 1-39.
[26] Y.-S. Ho, G. McKay, Pseudo-second order model for sorption processes, Process biochemistry, 34 (1999) 451-465.
[27] W. Weber, J. Morris, Proceeding of the International Conference on Water Pollution Symposium, Pergamon Press, Oxford, 2 (1962) 235-266.
[28] S. Allen, G. McKay, K. Khader, Intraparticle diffusion of a basic dye during adsorption onto sphagnum peat, Environmental pollution, 56 (1989) 39-50.

[29] C. Mangwandi, A.B. Albadarin, Y. Glocheux, G.M. Walker, Removal of ortho-phosphate from aqueous solution by adsorption onto dolomite, Journal of Environmental Chemical Engineering, 2 (2014) 1123-1130.
[30] N.S. Maurya, A.K. Mittal, P. Cornel, E. Rother, Biosorption of dyes using dead macro fungi: effect of dye structure, ionic strength and pH, Bioresource technology, 97 (2006) 512-521.
[31] I. Langmuir, The adsorption of gases on plane surfaces of glass, mica and platinum, Journal of the American Society, 40 (1918) 1361–1403.
[32] H.M.F. Freundlich, Over the adsorption in solution, The Journal of Physical Chemistry 57 (1906) 385–471.
[33] O. Redlich, D.L. Peterson, A useful adsorption isotherm, The Journal of Physical Chemistry, 63 (1959) 1024–1024.
[34] A.B. Albadarin, Z. Yang, C. Mangwandi, Y. Glocheux, G. Walker, M.N.M. Ahmad, Experimental design and batch experiments for optimization of Cr(VI) removal from aqueous solutions by hydrous cerium oxide nanoparticles, Chemical Engineering Research and Design, 92 (2014) 1354-1362.
[35] A. Mittal, J. Mittal, L. Kurup, Adsorption isotherms, kinetics and column operations for the removal of hazardous dye, Tartrazine from aqueous solutions using waste materials—bottom ash and de-oiled soya, as adsorbents, Journal of hazardous materials, 136 (2006) 567-578.
[36] L. Monser, N. Adhoum, Tartrazine modified activated carbon for the removal of Pb (II), Cd (II) and Cr (III), Journal of hazardous materials, 161 (2009) 263-269.
[37] W.S.W. Ngah, N.F.M. Ariff, M.A.K.M. Hanafiah, Preparation, characterization, and environmental application of crosslinked chitosan-coated bentonite for tartrazine adsorption from aqueous solutions, Water, Air, and Soil Pollution, 206 (2010) 225-236.
[38] M.A. Habila, Z.A. Alothman, R. Ali, A.A. Ghafar, M.S.E.-D. Hassouna, Removal of Tartrazine Dye onto Mixed-Waste Activated Carbon: Kinetic and Thermodynamic Studies, CLEAN – Soil, Air, Water, 42 (2014) 1824-1831.
[39] E. Daneshvar, A. Vazirzadeh, A. Niazi, M. Kousha, M. Naushad, A. Bhatnagar, Desorption of Methylene blue dye from brown macroalga: Effects of operating parameters, isotherm study and kinetic modeling, Journal of Cleaner Production, 152 (2017) 443-453.

380

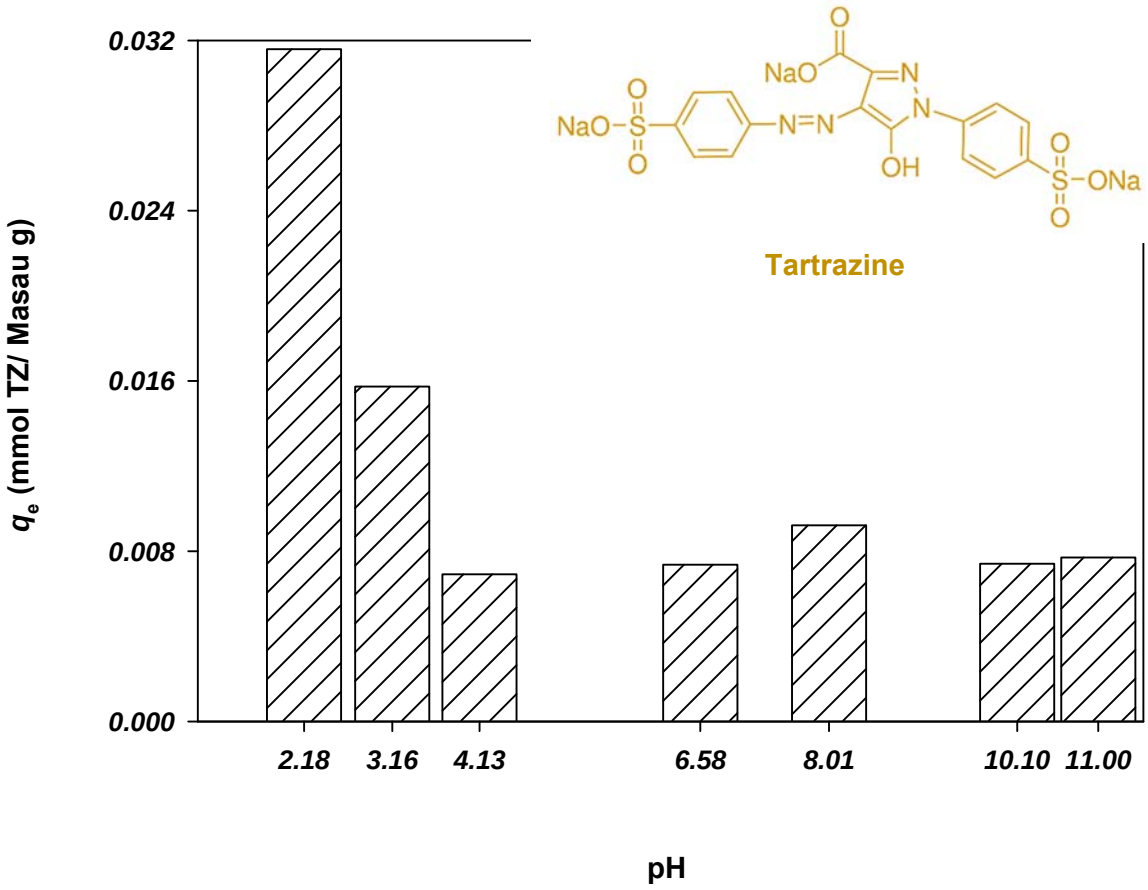

381

382 Figure 1: Effect of solution pH on the biosorption of tartrazine (TZ) onto masau stone (MS).

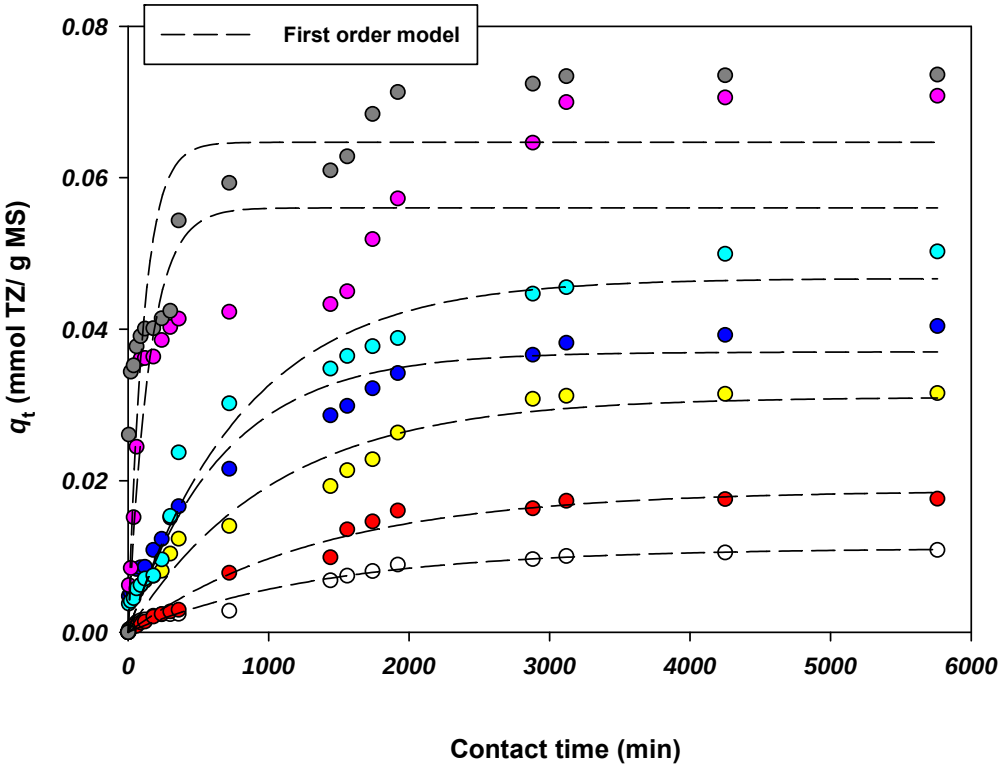
First order model
0.08
0.06
0.04
0.02
0.00
q_t (mmol TZ/ g MS)
0
1000
2000
3000
4000
5000
6000
Contact time (min)

383

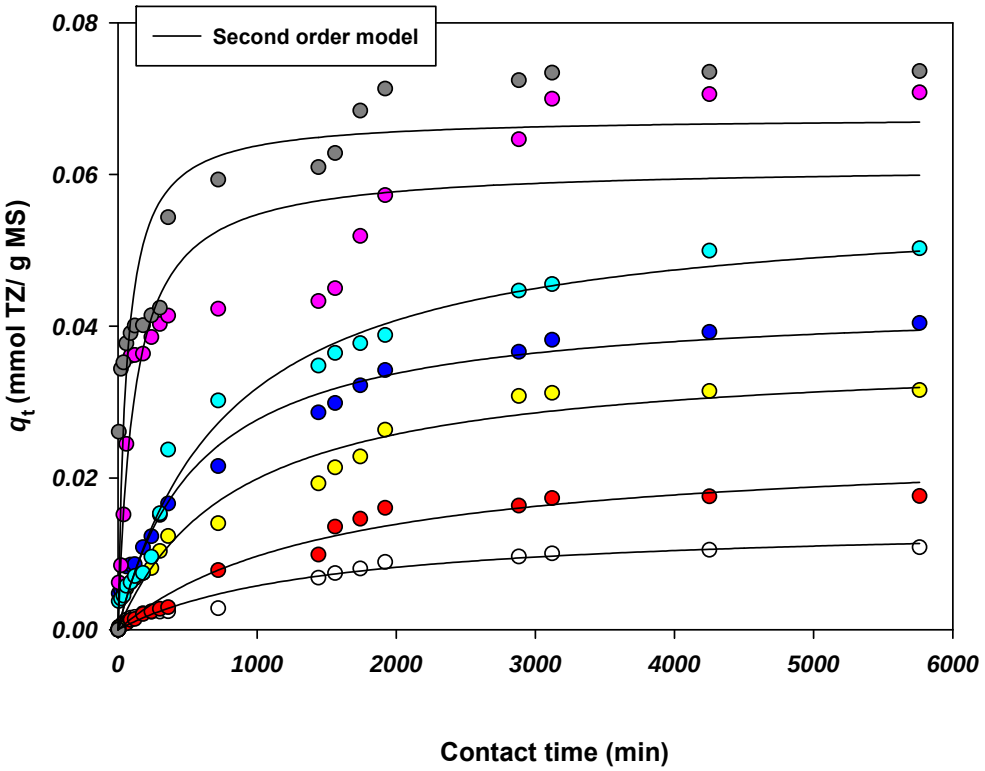
Second order model
0.08
0.06
0.04
0.02
0.00
q_t (mmol TZ/ g MS)
0
1000
2000
3000
4000
5000
6000
Contact time (min)

384

385

386 Figure 2: Biosorption kinetics of TZ removal onto MS at different concentrations (Increasing
387 C_o: 0.057, 0.102, 0.189, 0.313, 0.381, 0.600 and 0.861 mM) and fitting of pseudo first and
388 second order kinetics models.

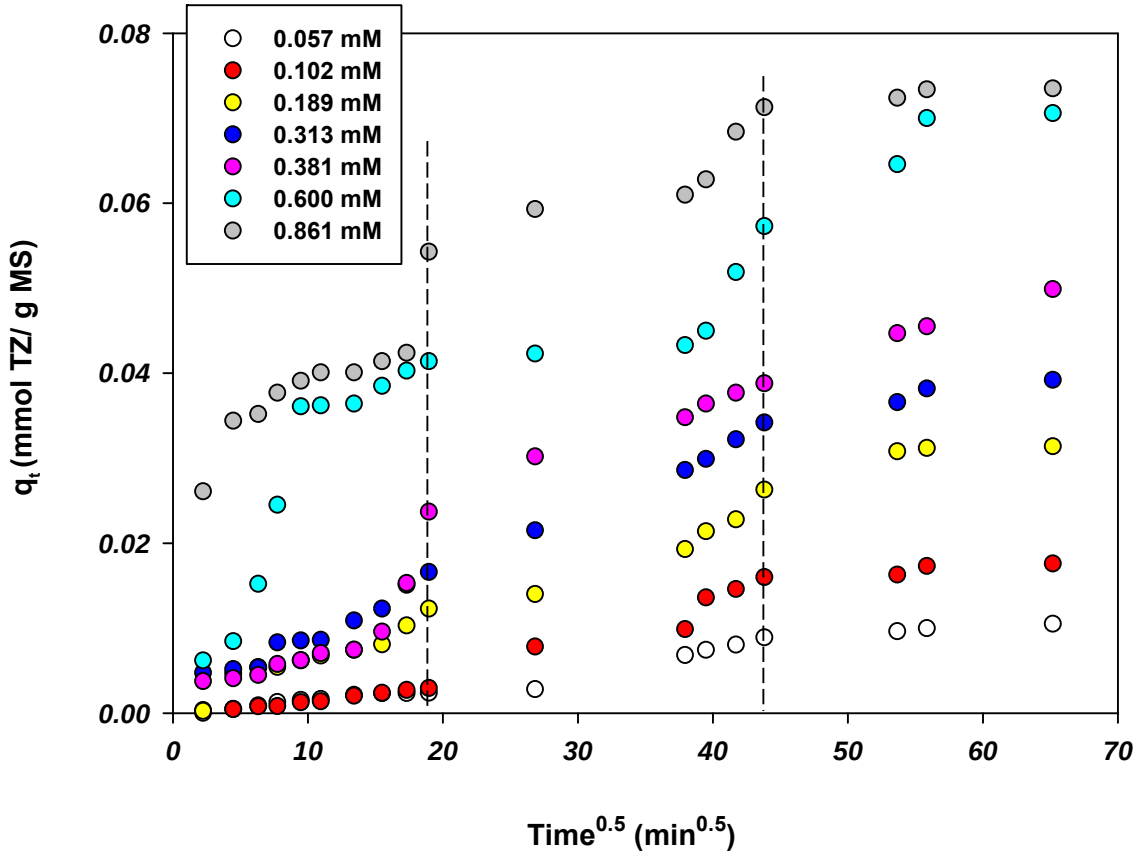

389

390 Figure 3: Intra-particle diffusion for TZ biosorption by MS.
391

392

393

394

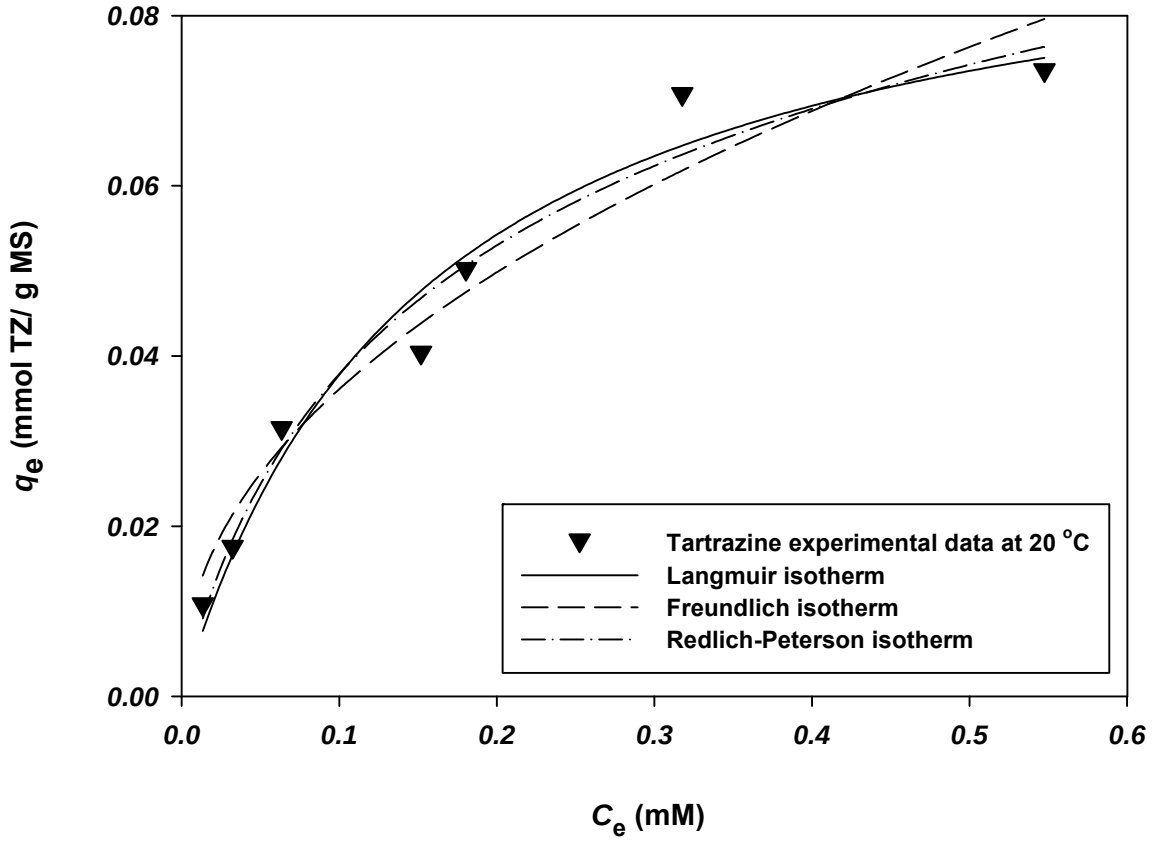

395

396 Figure 4: Equilibrium isotherm of TZ experiment data compared to equilibrium isotherm

397 correlations at 20ºC.

398

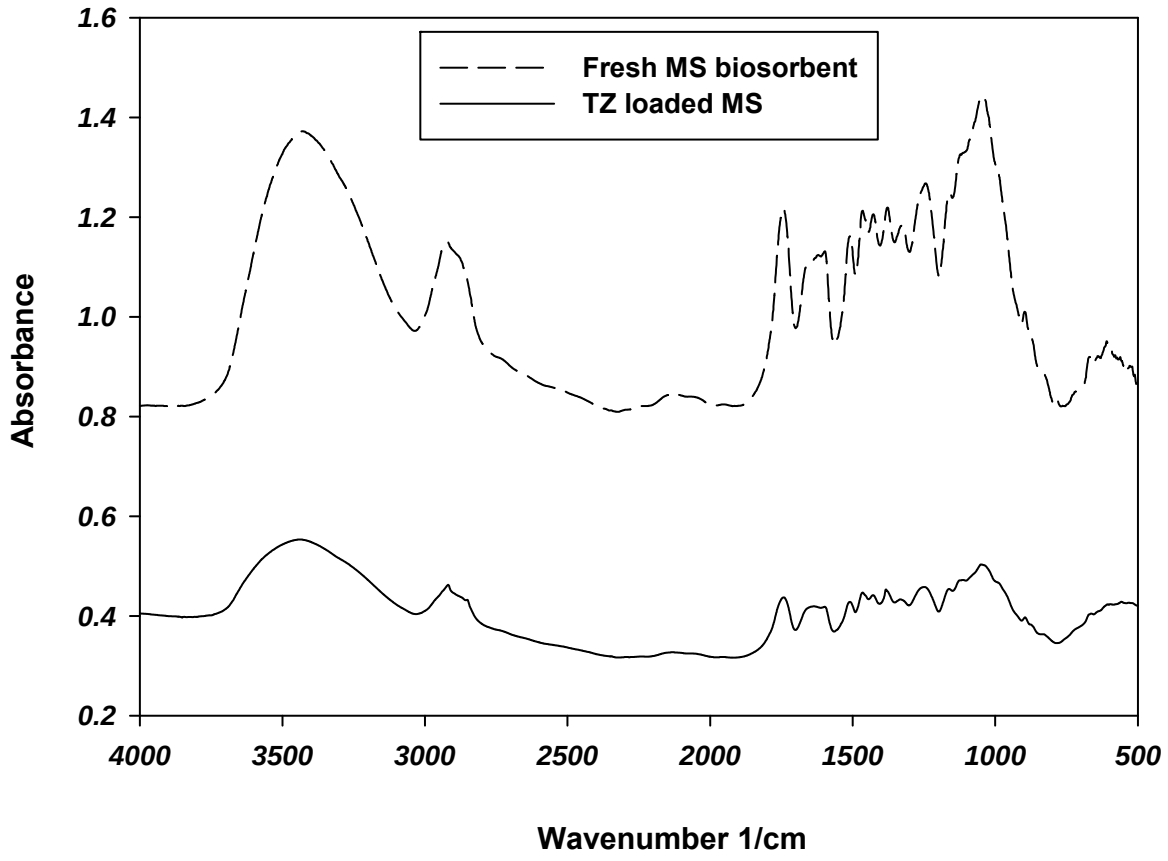

399

400 Figure 5: FTIR Spectra of fresh and loaded MS.

401

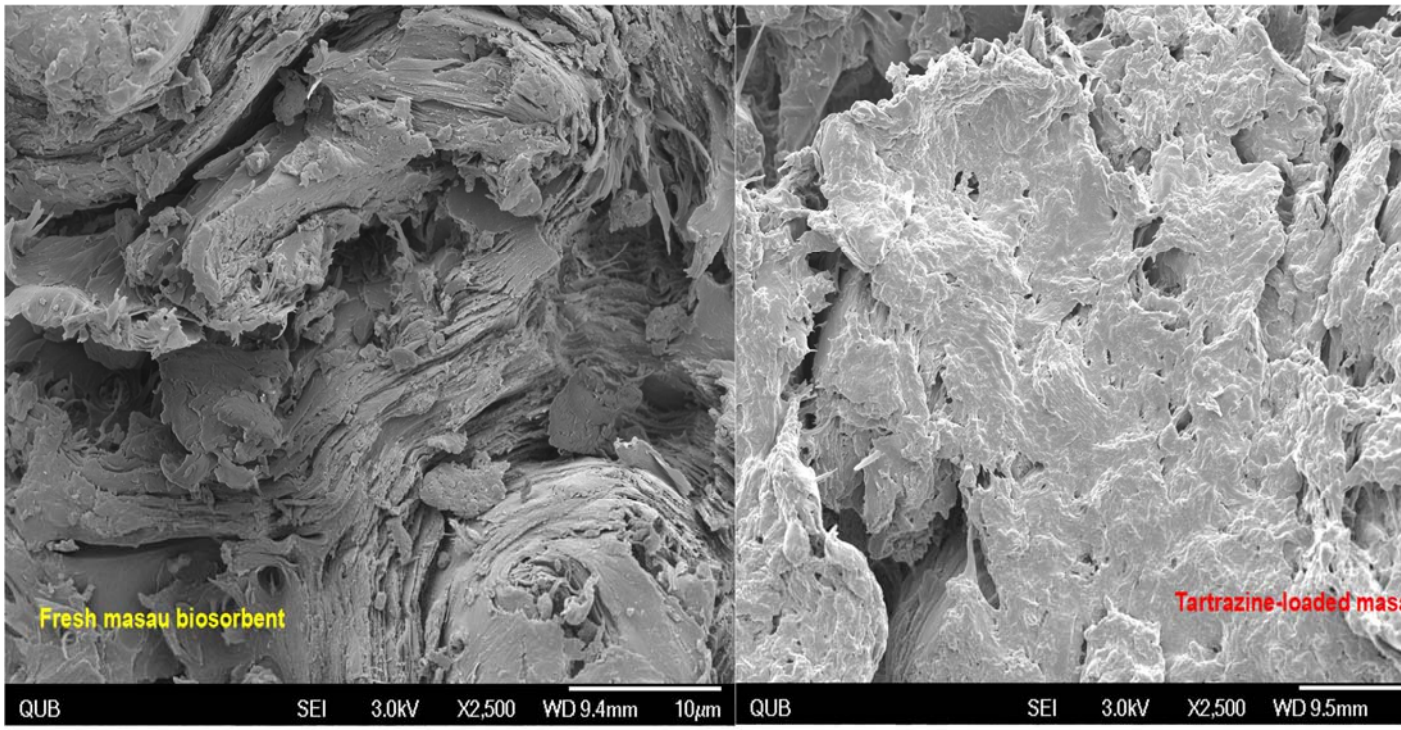

Figure 6: SEM images for MS before and after TZ biosorption.

Table 1: Pseudo first order and second order kinetic model constants for TZ biosorption onto MS.

	C_o (mM)		Pseudo first-order model			Pseudo second-order model		
		$q_{e,exp}$ (mmol/g)	$q_{e,cal}$ (mmol/g)	k_1 (1/min)	R^2	$q_{e,cal}$ (mmol /g)	k_2 (g/ mmol min)	R^2
TZ	**0.057 (mM)**	0.010	0.011	7.0×10^{-4}	0.988	0.014	0.048	0.988
	0.102 (mM)	0.017	0.018	7.0×10^{-4}	0.987	0.024	0.026	0.992
	0.189 (mM)	0.031	0.031	10.0×10^{-3}	0.970	0.036	0.032	0.978
	0.313 (mM)	0.040	0.037	15.0×10^{-3}	0.976	0.040	0.041	0.987
	0.381 (mM)	0.050	0.047	12.0×10^{-3}	0.985	0.056	0.022	0.991
	0.601 (mM)	0.071	0.056	6.7×10^{-3}	0.902	0.061	0.139	0.937
	0.861 (mM)	0.074	0.065	9.0×10^{-3}	0.804	0.067	0.248	0.887

Table 2: Intra-particle diffusion model parameters for the different diffusion phases.

	C_o (mM)	Intra-particle diffusion coefficients in mg/g.min$^{0.5}$					
		k_{1d}	R^2	k_{2d}	R^2	k_{3d}	R^2
TZ	**0.057 (mM)**	1.0×10^{-4}	0.944	3.0×10^{-4}	0.954	7.6×10^{-5}	0.979
	0.102 (mM)	2.0×10^{-4}	0.981	5.0×10^{-4}	0.934	8.0×10^{-5}	0.805
	0.189 (mM)	6.0×10^{-4}	0.898	6.0×10^{-4}	0.952	4.0×10^{-4}	0.741
	0.313 (mM)	7.0×10^{-4}	0.951	6.0×10^{-4}	0.972	2.0×10^{-4}	0.790
	0.381 (mM)	1.0×10^{-3}	0.728	6.0×10^{-4}	0.981	5.0×10^{-4}	0.997
	0.601 (mM)	4.2×10^{-3}	0.910	6.0×10^{-4}	0.844	6.0×10^{-4}	0.998
	0.861 (mM)	1.1×10^{-3}	0.803	5.0×10^{-4}	0.865	1.0×10^{-4}	1.000

Table 3: The Langmuir, Freundlich and Redlich-Peterson parameters and correlation coefficients for tartrazine (TZ) dye biosorption onto masau stone MS).

Model	Parameters	20ºC	30ºC	45ºC	60ºC
Langmuir isotherm	q_{max}	0.096	0.115	0.122	0.126
$q_e = \frac{q_{max} b C_e}{1 + b C_e}$		(51.3mg/g)	(61.4mg/g)	(65.1mg/g)	(67.4mg/g)
	b	6.460	6.609	8.237	12.70
	R^2	0.986	0.992	0.981	0.978
Freundlich isotherm	K_F	0.105	0.138	0.151	0.159
$q_e = K_F C_e^{1/n}$	$1/n$	0.556	0.505	0.454	0.401
	R^2	0.974	0.986	0.995	0.996
Redlich-Peterson isotherm	K_R	0.834	0.919	5.990	29.89
$q_e = \frac{K_R C_e}{1 + a_R C_e^{\beta}}$	a_R	8.246	6.917	40.30	189.2
	β	0.835	0.823	0.616	0.602
	R^2	0.985	0.993	0.994	0.996

Where: q_{max} (mmol/g); b (dm^3/mmol); K_F ((mg/g)·(mg/dm^3)^n); n (dimensionless); K_R (dm^3/g); a_R (dm^3/mg); and β (dimensionless).

Table 4: Comparison between various adsorbents for the removal of TZ.

Adsorbent	q_{max} (mg/g)	Reference
Hen feathers	64.1	[17]
Spirulina platensis	363.2	[20]
De-oiled soya	24.6	[33]
Bottom ash	12.6	[33]
Activated carbon	121.3	[34]
Crosslinked Chitosan-Coated Bentonite	294.1	[35]
Masau stone	51.3 (0.096 mmol/g)	This study

Table 5: Thermodynamic parameters

ΔH (kJ/mol)	ΔS (J/mol K)	ΔG (kJ/mol)			
		293 K	303 K	318 K	333 K
13.69	152.3	–31.15	–32.27	–34.46	–37.28

439
440
441
442